

NBSIR 75-671

# Examination of Piston Rod and Rod End From DC-8 Main Landing Gear Retract Cylinder Assembly

---

T. Robert Shives

Mechanical Properties Section  
Metallurgy Division  
Institute for Materials Research  
National Bureau of Standards  
Washington, D. C. 20234

February, 1975

Failure Analysis Report

Prepared for  
**Bureau of Aviation Safety**  
**National Transportation Safety Board**  
**Department of Transportation**  
**Washington, D. C. 20591**



NBSIR 75-671

**EXAMINATION OF PISTON ROD AND  
ROD END FROM DC-8 MAIN LANDING  
GEAR RETRACT CYLINDER ASSEMBLY**

---

T. Robert Shives

Mechanical Properties Section  
Metallurgy Division  
Institute for Materials Research  
National Bureau of Standards  
Washington, D. C. 20234

February, 1975

Failure Analysis Report

“This document has been prepared for the use of the Bureau of Aviation Safety, National Transportation Safety Board, Department of Transportation, Washington, DC. Responsibility for its further use rests with that agency. NBS requests that if release to the public is contemplated, such action be taken only after consultation with the Office of Public Affairs at the National Bureau of Standards.”

Prepared for  
Bureau of Aviation Safety  
National Transportation Safety Board  
Department of Transportation  
Washington, D. C. 20591



---

U. S. DEPARTMENT OF COMMERCE, Frederick B. Dent, Secretary

NATIONAL BUREAU OF STANDARDS, Richard W. Roberts, Director



## TABLE OF CONTENTS

SUMMARY	<u>Page</u>
1. GENERAL INFORMATION . . . . .	1
1.1 Reference . . . . .	1
1.2 Accident Information. . . . .	1
1.3 Parts Submitted . . . . .	1
2. PURPOSE . . . . .	1
3. RESULTS OF EXAMINATIONS AND TESTS . . . . .	1
3.1 Visual and Macroscopic Examination. . . . .	1
3.2 Chemical Analysis of the Corrosion Product. . . . .	2
3.3 Measurement of Thread Dimensions. . . . .	3
3.4 Fractographic Examination with the Scanning Electron Microscope . . . . .	3
3.5 Metallographic Examination. . . . .	4
3.6 Hardness Measurements . . . . .	5
4. DISCUSSION. . . . .	6
5. CONCLUSIONS . . . . .	7
6. ACKNOWLEDGEMENT . . . . .	8
TABLE 1. Thread Dimensions . . . . .	

### FIGURES

1. Piston rod and rod end as received at NBS . . . . .	
2. View of the rod end as received . . . . .	
3. View of the piston rod as received. . . . .	
4. View of the piston rod as received. . . . .	
5. Scanning electron fractograph showing part of the undamaged fracture surface. . . . .	

FIGURES (continued)

6. Scanning electron fractograph showing a typical area of the undamaged part of the fracture surface of the piston rod. . . . .
7. Scanning electron fractograph showing a typical area of the piston rod fracture surface. . . . .
8. Scanning electron fractograph where the fracture intersects the threads. . . . .
9. As-polished longitudinal sections through the piston rod showing the thread profile. . . . .
10. Longitudinal section through the piston rod showing the roots of two threads in areas not opposite the keyway in the mating rod end. . . . .
11. Etched longitudinal section through piston rod away from the fracture showing part of one thread . . . .
12. Etched longitudinal section through piston rod away from the fracture . . . . .
13. Longitudinal section through the piston rod showing the fracture profile in an undamaged region of the fracture. . . . .
14. Longitudinal section through the piston rod showing the fracture profile in a mechanically damaged region of the fracture . . . . .
15. As-polished longitudinal section through the piston rod showing an average inclusion content. . . . .
16. As-polished longitudinal sections through the rod end showing the thread profile. . . . .
17. As-polished longitudinal section through the rod end. . . . .
18. Etched longitudinal section through the rod end showing part of one of the threads . . . . .
19. Etched longitudinal section through the rod end showing typical microstructure. . . . .
20. As-polished longitudinal section through the rod end showing an average inclusion content. . . . .

## SUMMARY

A failed piston rod and rod end from a DC-8 aircraft main landing gear retract cylinder assembly was submitted to the NBS Mechanical Properties Section for examination. The threads of both of the mating parts were severely corroded and had suffered rather severe mechanical damage. The mechanical damage of the threads appeared to be the result of the failure rather than the cause of the failure. A large portion of the fracture surface had been damaged by an apparent rubbing action. Dimpled rupture was the primary feature exhibited by the undamaged portion of the fracture surface. An anti-seize compound with a molybdenum disulfide base was reportedly used on the threads when the components were in service, but no molybdenum was detected in a chemical analysis of the corrosion product. Of those thread dimensions checked, the root radius of the rod end did not appear to meet specifications.



Examination of Piston Rod and Rod End from DC-8  
Main Landing Gear Retract Cylinder Assembly

1. GENERAL INFORMATION

1.1 Reference

Bureau of Aviation Safety, National Transportation Safety Board, Department of Transportation, Washington, DC. This investigation was requested by Mr. Jerry A. Houck in a letter dated July 26, 1974.

1.2 Accident Information

The submitted parts were from a Braniff DC-8 aircraft involved in an accident at Tocumen, Panama, on May 19, 1974.

1.3 Parts Submitted

Portions of a piston rod and the mating rod end from a main landing gear retract cylinder assembly from the above mentioned aircraft were submitted to the NBS Mechanical Properties Section for examination. A nut was attached to the rod end. The parts are shown as received in figure 1. The piece of material missing from the piston rod and a key fitted to the rod end were not submitted.

2. PURPOSE

The Bureau of Aviation Safety requested that the NBS Mechanical Properties Section perform a failure analysis of the submitted parts with emphasis on (1) an analysis of the corrosion product in the threaded regions and (2) a measurement of the thread dimensions.

3. RESULTS OF EXAMINATIONS AND TESTS

3.1 Visual and Macroscopic Examination

The threaded regions of both the piston rod and the rod end were covered with what appeared to be a rather heavy corrosion product. Both sets of threads had suffered extensive mechanical damage. Part of the threaded region of the rod end is shown in figure 2. In addition to the corrosion product and the mechanical damage, parts of some of the threads from the mating piston rod can be seen still attached to the rod end (arrows, figure 2).

Part of the threaded region of the piston rod is shown in figure 3. The fracture surface and the damaged and corroded threads can be seen. A piece of the rod which had separated at the fracture was not submitted for examination. Portions of several threads are missing. The arrows in figure 3 indicate the location of the transition from corroded to essentially non-corroded regions. Another view of the piston rod is shown in figure 4. The fracture surface had been subjected to severe mechanical damage except for the area indicated by arrow A where the fracture path was parallel to the longitudinal axis of the rod. Discoloration of the fracture surface in some areas of the damaged region indicates that the fracture surface may have been subjected to temperatures high enough to produce an oxide with a straw or blue color. In many places, the fracture surface is smooth and somewhat shiny and has the appearance of having been rubbed. Where it had not been damaged, the fracture surface has a "woody" or "layered" appearance. The piston rod was deformed in the vicinity of the fracture. This deformation can be seen in figure 4 in the region designated by arrow B. Another indication of the deformation is the cracked chromium plating on the outside surface of the rod in the vicinity of the fracture. This is especially evident in the area designated C in figure 4.

In the region from arrow C to approximately the location of arrow D, there is a pronounced lip, as if the outside portion of the fracture surface had been subjected to a compressive deformation or a pronounced downward wiping.

### 3.2 Chemical Analysis of the Corrosion Product

A chemical analysis of the corrosion product on the threads of the piston rod was made by the NBS Analytical Chemistry Division using electron microprobe techniques. The semi-quantitative results are as follows:

<u>Element</u>	<u>Percent (weight)</u>
Iron	50
Chromium	3
Sulfur	<1
Silicon	<1
Aluminum	<1
Nickel	<1
Carbon	<1

The remaining major constituent was oxygen. Carbon and oxygen were the only elements with atomic numbers less than that of sodium that were checked. Elements with atomic numbers higher than that of sodium were analyzed with a sensitivity of about 0.1%.

### 3.3 Measurement of Thread Dimensions

According to Douglas Aircraft Company drawings, the threads of the piston rod and the rod end were to be rolled. The dimensions of the 1 3/8 - 12 threads were to be in conformance with Military Specification MIL-S-8879A. The dimensions and permissible deviations for the pitch, half angle, and root radius as given in MIL-S-8879A are listed in part "a" of Table 1.

The corroded and damaged condition of the threads of both the piston rod and the rod end made accurate measurement of the thread dimensions very difficult. The threads of the piston rod appeared to be in the best condition in a region that had apparently been opposite a keyway in the mating rod end. A longitudinal section was taken through this region of the rod so that the thread profile was as nearly perpendicular to the tangent to the rod at this point as practicable. The pitch was measured for a series of seven consecutive threads. The results of these measurements are given in part "b" of Table 1. The average pitch based on the total accumulated distance across the seven threads was 0.0843 inch. Because of the condition of the threads, the half angle was measured for only one thread and the root radius was determined for only three threads. The results of the half angle and root radius measurements are also given in part "b" of Table 1. The estimated accuracy of the measurements presented in part "b" of Table 1 is as follows: pitch,  $\pm 0.003$  inch; half angle, no better than  $\pm 1^\circ$ ; root radius,  $\pm 0.002$  inch.

The threads of the rod end appeared to be in the best condition under the nut that was attached to it when it was submitted for examination. In a manner similar to that described above, a longitudinal section was taken through the rod end where the nut was attached. The pitch, half angles, and root radii were measured for eight consecutive threads, six of which were under the nut. The results of these measurements are given in part "c" of Table 1. The estimated accuracy of these measurements is as follows: pitch,  $\pm 0.002$  inch; half angle, no better than  $\pm 2^\circ$ ; root radius,  $\pm 0.002$  inch. The pitch based on the total accumulated distance across the eight threads was 0.0835 inch.

### 3.4 Fractographic Examination with the Scanning Electron Microscope

Part of the relatively undamaged portion of the fracture surface in the region indicated by arrow B in figure 4 was examined with the scanning electron microscope. A low magnification fractograph with the longitudinal direction of the piston

rod in the horizontal position is shown in figure 5. The "woody" or "layered" appearance of the fracture is evident. At higher magnifications, it is seen that this region of the fracture surface exhibits dimpled rupture as the primary fracture mode. Fractographs showing typical areas of the relatively undamaged portion of the fracture surface appear in figures 6 and 7. There may be some corrosion product on the fracture surface in the area shown in figure 7.

In figure 8, part of the fracture surface intersecting the threads is shown. Mechanical damage and the generally deteriorated condition of the threads can be seen.

### 3.5 Metallographic Examination

As-polished longitudinal sections through the piston rod showing the thread profile appear in figures 9a and 9b. The profile shown in figure 9a is in a region that (apparently) had been opposite the keyway in the mating rod end. The threads appeared to be in better condition in this region than elsewhere on the rod. Even so, the threads exhibited rather severe deterioration. In figure 9b, a thread profile exhibiting the representative condition of the threads away from the region opposite the rod end keyway is shown. The threads here have suffered extensive corrosive attack and mechanical damage. In figure 10, the roots of two of the threads in a region not opposite the keyway are shown at higher magnification. There is a considerable amount of corrosion product in evidence.

A field from an etched longitudinal section through the rod showing part of one thread in an area away from the fracture appears in figure 11. The results of mechanical damage as manifested in microscopic deformation at the tip of the thread is evident. The results of corrosive attack can also be seen. In the particular field shown in figure 11, several stringer type inclusions are present. The inclusion content in this field appeared to be higher than the average for the material. The microstructure of the rod material away from the fracture shown in figure 11, and at higher magnification in another area adjacent to the outside surface of the rod in figure 12, consists primarily of tempered martensite.

The fracture profile in a relatively undamaged region of the fracture (indicated by arrow A, figure 4) and in a mechanically smoothed region of the fracture (close to arrow D, figure 4) are shown in figures 13 and 14, respectively. The profile in the undamaged region is jagged, and there is no clear evidence of deformation. The steel has been smeared over the chromium plating at the left of the figure. The microstructure appears to be somewhat finer adjacent to the fracture.

A field from an as-polished longitudinal section through the piston rod in an area that had been opposite the rod end keyway exhibiting an average inclusion content for the material examined is shown in figure 15.

As-polished longitudinal sections showing the thread profile of the rod end in an area under the nut and in an area not under the nut appear in figures 16a and 16b, respectively. It is quite evident that the threads under the nut were in better condition than those not under the nut. The threads not under the nut had suffered both mechanical damage and rather severe corrosive attack. The threads under the nut had suffered less severe corrosive attack and essentially no mechanical damage. Examples at higher magnification of a thread under the nut and one not under the nut are shown in figures 17a and 17b, respectively. The results of corrosive attack are evident in different degrees of severity in both figures, and rather severe mechanical damage can be seen in figure 17b. Part of a thread not under the nut in an etched longitudinal section of the rod end is shown in figure 18. Microscopic deformation is evident. A field from an etched longitudinal section is shown at higher magnification in figure 19. The microstructure consists primarily of tempered martensite.

A field from an as-polished longitudinal section showing the average inclusion content for the rod end material appears in figure 20. This steel appears to be somewhat cleaner than the steel of the piston rod.

### 3.6 Hardness Measurements

Rockwell hardness measurements were made on transverse sections through the piston rod and the rod end. Based on four measurements each, the average hardness values for the piston rod and for the rod end were  $R_C$  38 and 42 1/2, respectively. These hardness values are approximately equivalent to ultimate tensile strengths of 170 ksi for the piston rod and 197 ksi for the rod end. Douglas Aircraft Company drawings call for tensile strengths of 150 to 180 ksi for the rod and 180 to 200 ksi for the rod end.

Knoop microhardness measurements at a load of 500 grams were made on the piston rod in a longitudinal section that intersected the fracture in a damaged region. The average hardness at locations 0.003 inch and further from the fracture was KHN 410, which corresponds approximately to  $R_C$  41. Adjacent to the fracture, however, the material was much softer. At distances of 0.002 and 0.001 inch from the fracture, the hardness values were KHN 239 and 264, respectively. These values correspond approximately to  $R_B$  98 at 0.002 inch and  $R_C$  23 at 0.001 inch from the fracture.

#### 4. DISCUSSION

Where the threads of the piston rod and the rod end had been in contact, the threads were generally badly corroded and exhibited severe mechanical damage. There was a considerable amount of corrosion product in the threads of both parts. This corrosion product extended only slightly beyond the threaded regions. The corrosion of the rod end threads under the nut was much less severe than that of the threads not under the nut.

On the other hand, the nut was solidly "frozen" in place, which implies that before failure, the rod end was also frozen into the piston rod. The mechanical damage incurred by the threads appears to be the result, rather than the cause, of the failure.

It was reported that, in service, a molybdenum disulfide base anti-seize compound was supposed to have been applied to the threaded joint between the piston rod and the rod end. It may be significant that molybdenum was not detected in the chemical analysis of the corrosion product on the threads. Sulfur in amounts of 1% or less was detected.

The deteriorated and damaged condition of the threads made the accurate measurement of thread dimensions very difficult. In Table 1, all pitch measurements except one for the piston rod appear to meet specifications, when considering the estimated accuracy of the measurements. The apparent discrepancy for the one measurement (no. 7, Table 1, part b) may be due to both corrosion and mechanical damage and therefore may not be real. There is no sound evidence to indicate that the pitch of any of the threads failed to meet specifications at the time the parts were put into service.

Again, considering the permitted deviation and the estimated accuracy of measurement, all of the half angles measured except one (no. 1, Table 1, part c) appeared to meet specifications. The one which did not appear to meet specifications measured about one degree greater than acceptable, but the thread conditions may be responsible for this apparent discrepancy.

There does appear to be a real discrepancy in the root radii dimensions of the threads of the rod end. In every case where this dimension was checked, the measured value of the root radius is not within the specified range, even when considering the estimated accuracy of measurement.

The features of the undamaged portion of the fracture indicated that the fracture was ductile. The damaged portion

of the fracture surface appeared to have rubbed against something which made it relatively smooth. This part of the fracture was discolored in places and had the appearance of having been subjected to temperatures high enough to form straw or bluish colored oxides. Hardness measurements indicated that the material adjacent to the fracture was softer than that away from the fracture. This change in hardness also indicates a possible heat effect.

The general appearance of the fracture surface, the overall shape of the fracture path, and particularly the lip under the lowest portion of the fracture surface, are all consistent with the failure having occurred by the rod end breaking out through the wall of the piston rod. This is visualized to have occurred by a rotating motion of the rod about a transverse axis. However, the mode of failure is not consistent with the lack of serious mechanical damage on the bottom portion of the rod end. In addition, there is no obvious relation between this failure mode and the corroded condition of the threads. The cause of failure is not clear.

Based on hardness values from measurements away from the fracture, the ultimate tensile strength of the material from both the piston rod and the rod end met specifications.

The material from both parts was, on the average, relatively clean with few inclusions, but there was at least one area in a longitudinal section through the piston rod that contained a significantly higher concentration of inclusions.

## 5. CONCLUSIONS

1. The mechanism of the piston rod fracture appeared to be ductile overload.
2. The primary fracture mode was dimpled rupture.
3. Part of the fracture surface had suffered rather severe mechanical damage and appeared to have been subjected to a temperature sufficiently high to cause discoloration and a decrease in hardness in adjacent material.
4. The threads of both the piston rod and the rod end were severely corroded where the two parts had been in contact. The threads were corroded elsewhere, but less severely.

5. The threads of both the piston rod and the rod end had suffered rather severe mechanical damage. This damage appeared to be the result of the failure. The damage was more severe in the piston rod than in the rod end.
6. Of those thread dimensions checked, only the root radii of the rod end appeared not to meet specifications.
7. Molybdenum was not detected in a chemical analysis of the corrosion product in the threads.
8. Based on hardness measurements, the ultimate tensile strength of both the piston rod and the rod end met specifications.
9. At least one area of a longitudinal section through the piston rod contained a significantly higher than average concentration of inclusions.

#### 6. ACKNOWLEDGEMENT

The specimen preparation work, photography, and hardness measurements were performed by Mr. L. C. Smith of the NBS Mechanical Properties Section.

Table 1. Thread Dimensions

a. Selected Specified Dimensions and Tolerances from MIL-S-8879A

	Pitch	Allowable Lead	Half Angle	Allowable Half Angle Deviation	Root Radius
Internal Threads	0.083333 in	0.00141 in	30°	1° 07'	
External Threads	0.083333 in	0.00109 in	30°	0° 52'	0.0125 in min - 0.0150 in max

b. Results of Piston Rod Dimension Measurements

Thread	Pitch (in)	Half Angles	Root Radius (in)
1	0.086	29° 14' 30° 31'	0.010
2	0.081		0.010
3	0.087		0.010
4	0.080		
5	0.086		
6	0.082		
7	0.088		

c. Results of Rod End Dimension Measurements

1	0.083	33° 44' 30° 12'	0.006
2	0.084	29° 20' 32° 47'	0.007
3	0.084	31° 33' 31° 52'	0.007
4	0.082	29° 56' 29° 50'	0.007
5	0.084	30° 41' 29° 43'	0.007
6	0.083	30° 45' 30° 15'	0.007
7	0.084	29° 53' 29° 45'	0.008
8	0.084	29° 47' 29° 20'	0.007





Figure 1. Piston rod (left) and rod end (right) as received at NBS. There is a nut attached to the rod end. The keyway in the rod end is indicated by the arrow. X3/4





Figure 2. View of the rod end as received. Thread damage is evident. Parts of some of the threads of the mating piston rod can be seen. Arrows indicate examples of regions where parts of threads from the mating piston rod are still attached. X2





Figure 3. View of the piston rod as received. The fracture surface and portions of the corroded and damaged threads can be seen. The arrows indicate the approximate location of a transverse plane through the rod beyond which there is essentially no corrosion product. X2



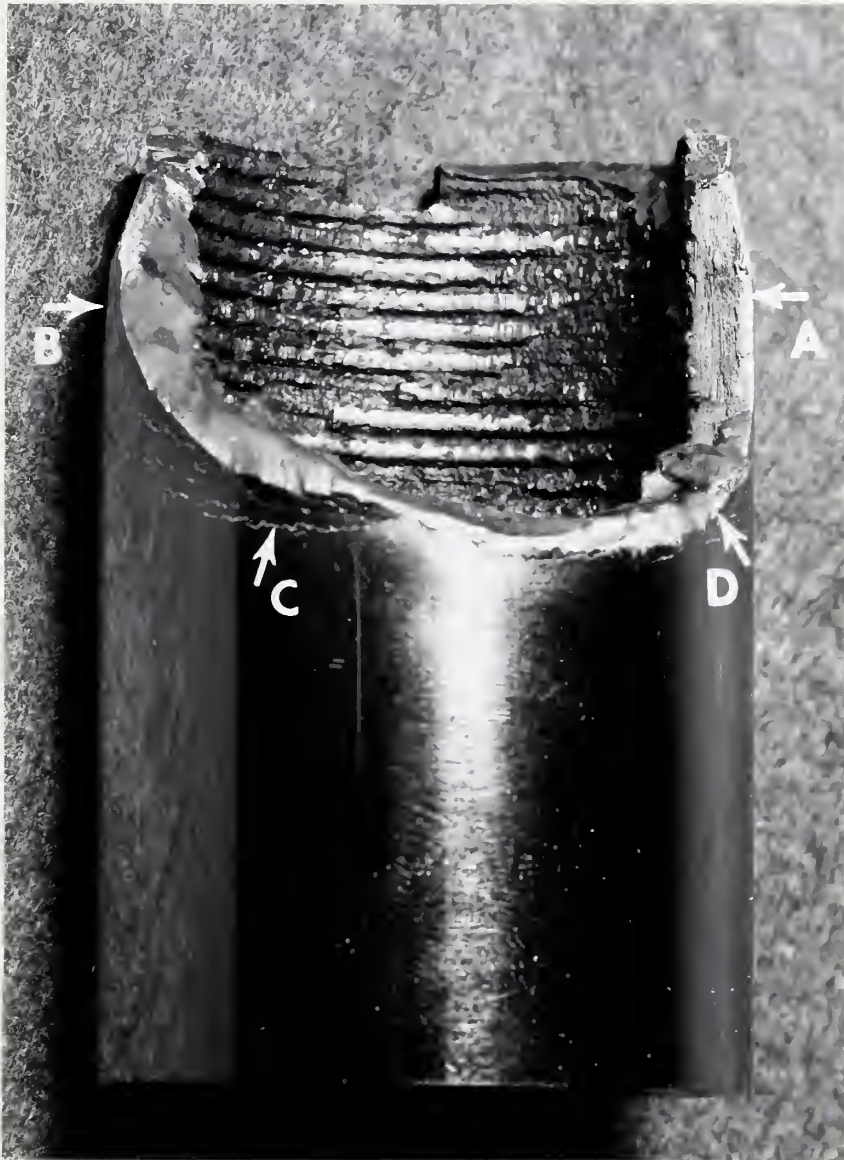


Figure 4. View of the piston rod as received showing most of the fracture surface. Except for the longitudinal part of the fracture (arrow A), the fracture surface was rather severely damaged. Arrow B indicates a region of macroscopic deformation. Arrow C indicates an example of cracks in the chromium plating. There is a pronounced lip along the fracture extending approximately from C to D. X2





Figure 5. Scanning electron fractograph showing part of the undamaged fracture surface in the area designated by arrow B in figure 4. The longitudinal axis of the piston rod is horizontal. X17

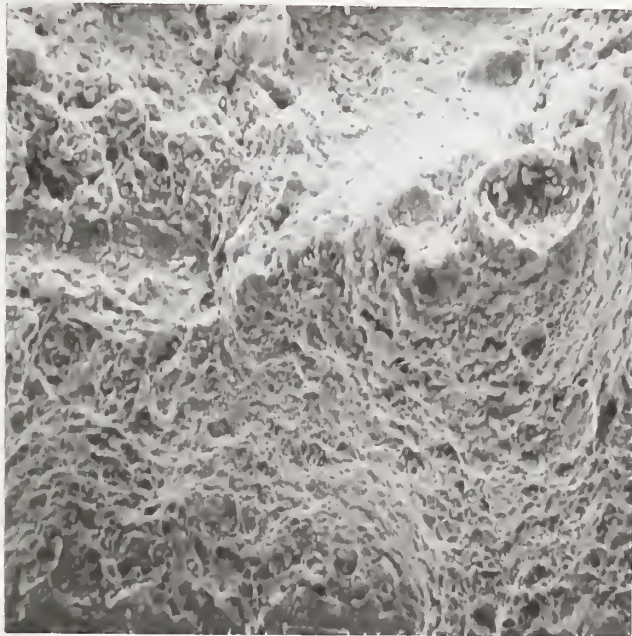


Figure 6. Scanning electron fractograph showing a typical area of the undamaged part of the fracture surface of the piston rod. The primary feature exhibited is dimpled rupture. X825



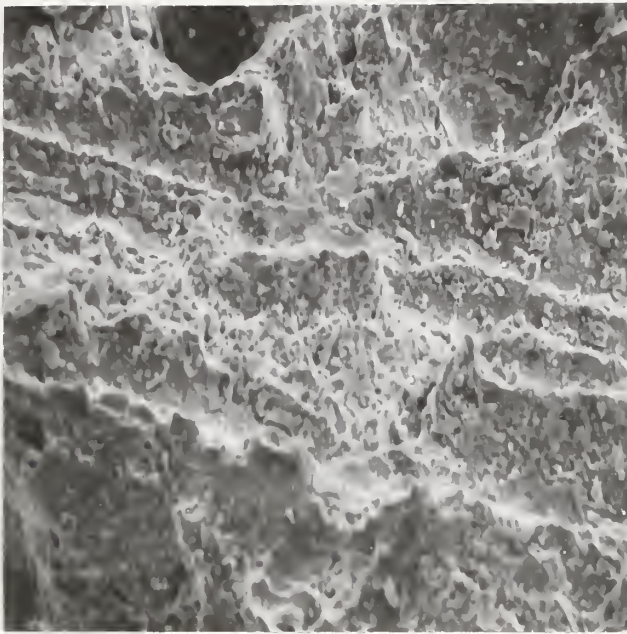


Figure 7. Scanning electron fractograph showing a typical area of the piston rod fracture surface. The primary feature exhibited is dimpled rupture. There may be some corrosion product on the surface. There is some evidence of the "layered" appearance that can be seen in figure 5. X825

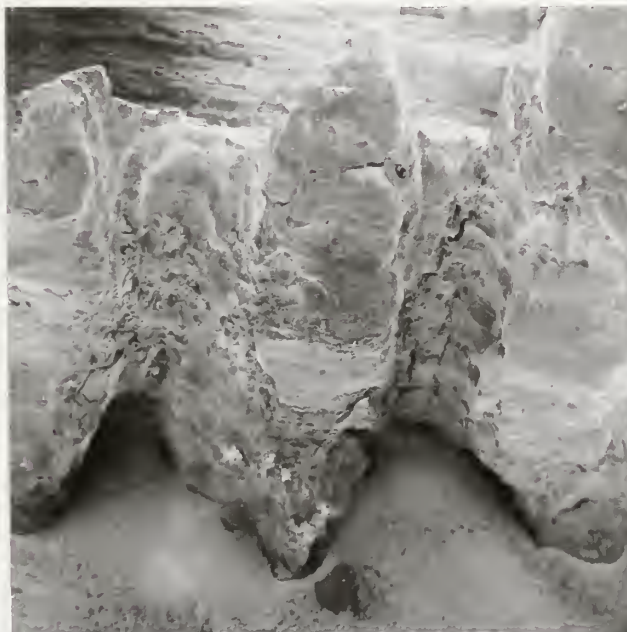


Figure 8. Scanning electron fractograph where the fracture intersects the threads. Mechanical damage and the deteriorated condition of the threads are evident. X18





a



b

Figure 9. As-polished longitudinal sections through the piston rod showing the thread profile. The threads appear white. X12

- a. Area apparently opposite the keyway in the mating rod end. The threads are corroded, but do not appear to be mechanically damaged.
- b. Area not opposite the keyway in the mating rod end. Threads are both corroded and mechanically damaged.





a



b

Figure 10. Longitudinal section through the piston rod showing the roots of two threads in areas not opposite the keyway in the mating rod end. A considerable amount of corrosion product is evident. Threads appear white. As-polished. X100



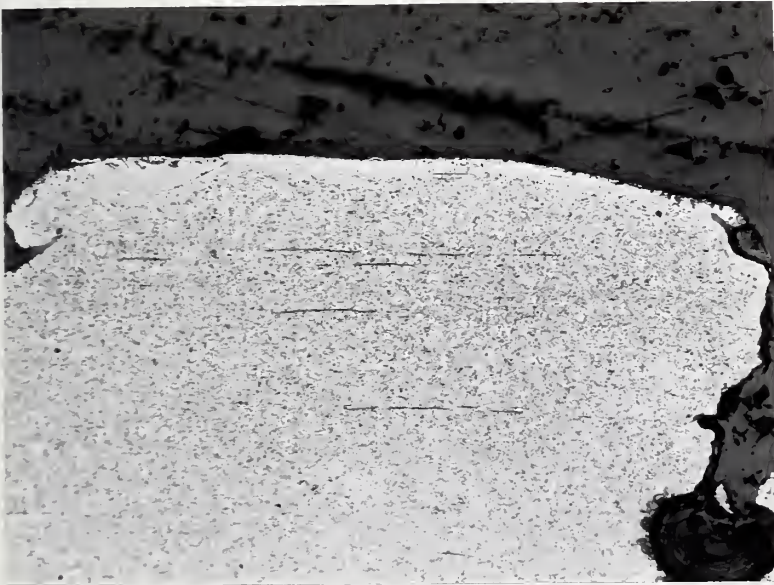


Figure 11. Etched longitudinal section through piston rod away from the fracture showing part of one thread (left). Deformation is evident at the tip. Etchant: 4% picral X80



Figure 12. Etched longitudinal section through piston rod away from fracture. The chromium plating on the outside surface of the rod is the light layer at the left. The microstructure consists of tempered martensite. Etchant: 4% picral X200



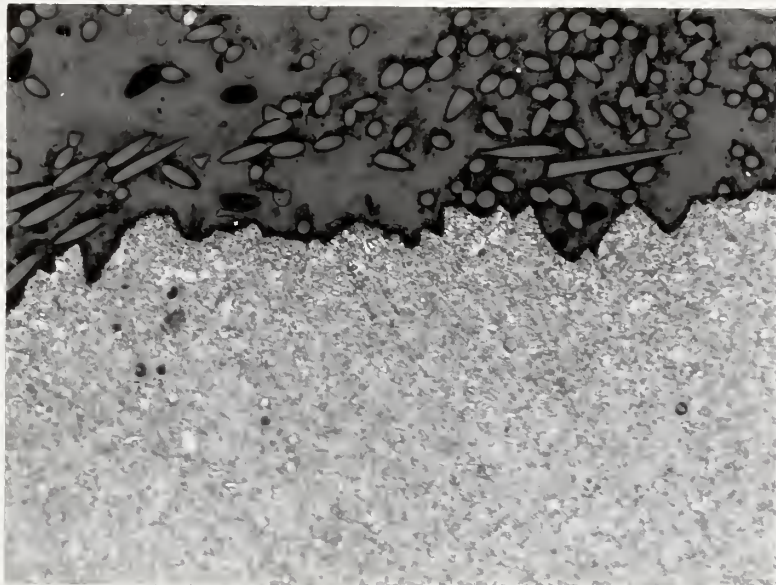


Figure 13. Longitudinal section through the piston rod showing the fracture profile in an undamaged region of the fracture.  
Etchant: 4% picral X200



Figure 14. Longitudinal section through the piston rod showing the fracture profile adjacent to the outside surface in a mechanically damaged region of the fracture.  
Etchant: 4% picral X200





Figure 15. As-polished longitudinal section through the piston rod showing an average inclusion content for the rod material examined. X100





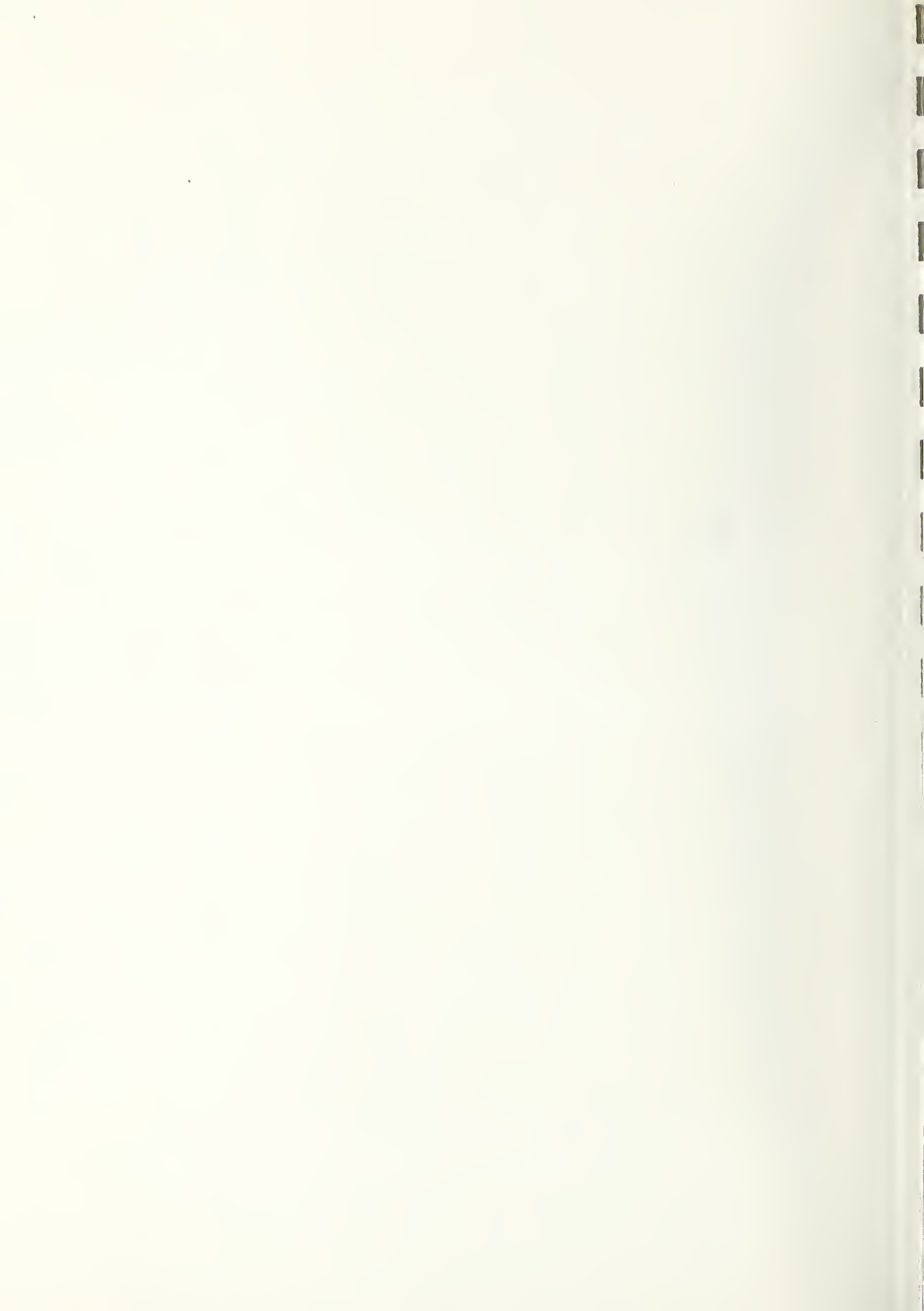
a



b

Figure 16. As-polished longitudinal sections through the rod end showing the thread profile. The threads appear white. X12

- a. Rod end threads under the nut. The rod end is on the right and the nut is on the left. The threads appear to have suffered some corrosive attack, but no mechanical damage.
- b. Rod end threads not under the nut. The threads appear to have been severely corroded and mechanically damaged.





a

b

Figure 17. As-polished longitudinal section through the rod end. X50

- a. Root of thread under the nut. Both the rod end and the nut appear white. The rod end is at the right. There is evidence of corrosive attack, but not of mechanical damage.
- b. Part of the threaded region not under the nut. The rod end appears white. There is evidence of both corrosive attack and mechanical damage.

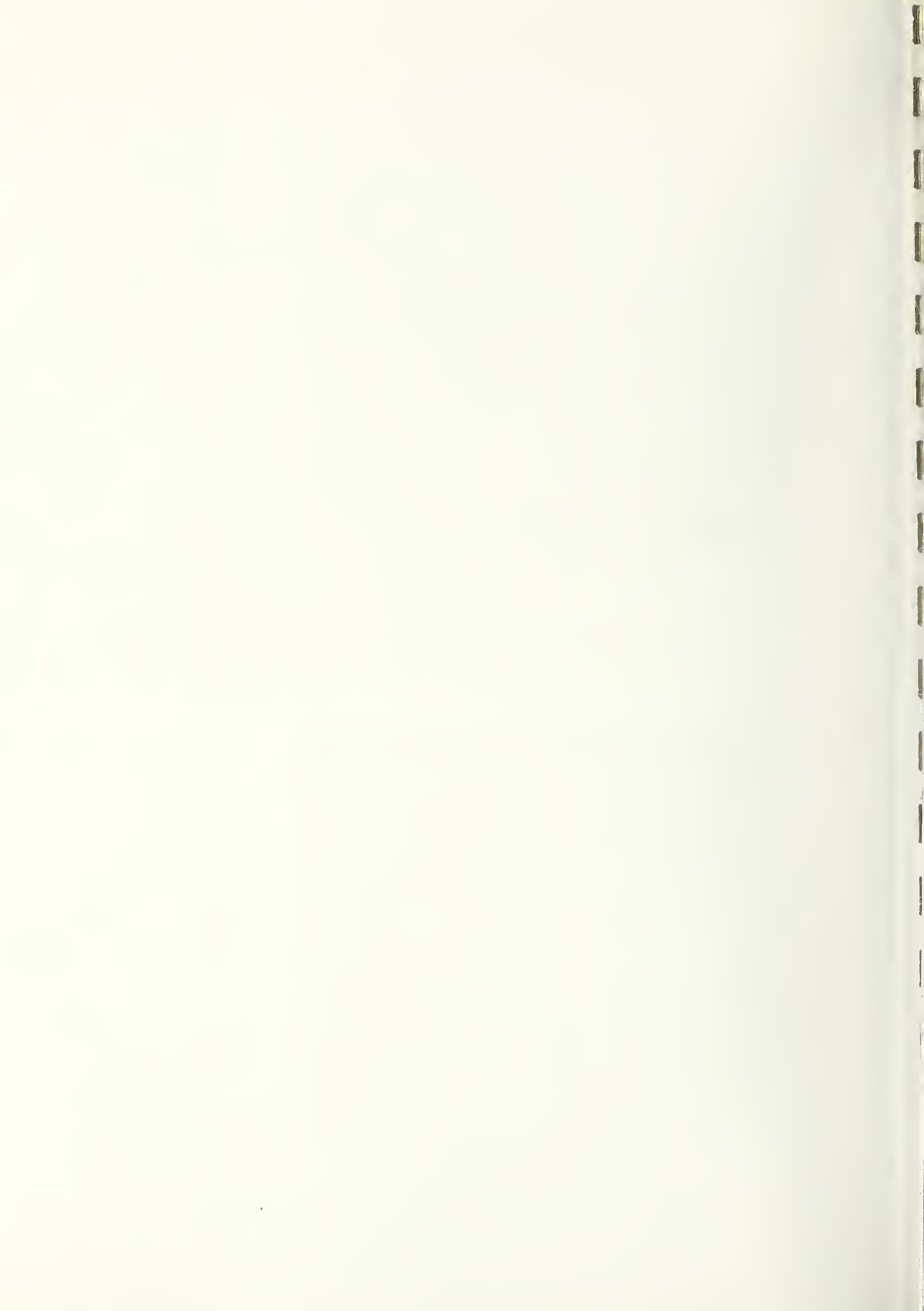




Figure 18. Etched longitudinal section through the rod end showing part of one of the threads. Deformation is evident. Etchant: 4% picral X100



Figure 19. Etched longitudinal section through the rod end showing typical microstructure. The microstructure consists primarily of tempered martensite. Etchant: 4% picral X200



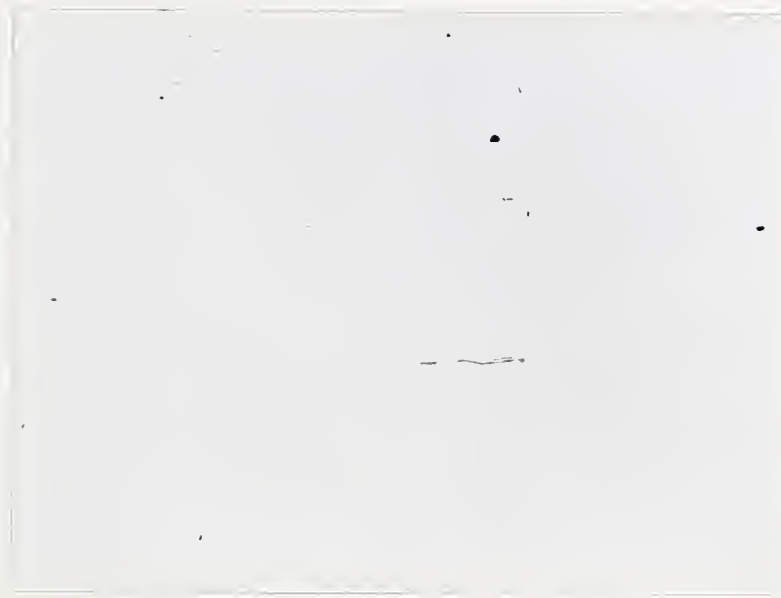


Figure 20. As-polished longitudinal section through the rod end showing an average inclusion content for the rod end material examined.  
X100



U.S. DEPT. OF COMM. BIBLIOGRAPHIC DATA SHEET	1. PUBLICATION OR REPORT NO. NBSIR 75-671	2. Gov't Accession No.	3. Recipient's Accession No.
4. TITLE AND SUBTITLE EXAMINATION OF PISTON ROD AND ROD END FROM DC-8 MAIN LANDING GEAR RETRACT CYLINDER ASSEMBLY		5. Publication Date February 1975	6. Performing Organization Code
7. AUTHOR(S) T. R. Shives	8. Performing Organ. Report No. NBSIR 75-671		
9. PERFORMING ORGANIZATION NAME AND ADDRESS NATIONAL BUREAU OF STANDARDS DEPARTMENT OF COMMERCE WASHINGTON, D.C. 20234		10. Project/Task/Work Unit No.	11. Contract/Grant No.
12. Sponsoring Organization Name and Complete Address (Street, City, State, ZIP) Bureau of Aviation Safety National Transportation Safety Board, DOT Washington, D.C. 20591		13. Type of Report & Period Covered Failure Analysis Report	14. Sponsoring Agency Code
15. SUPPLEMENTARY NOTES			
16. ABSTRACT (A 200-word or less factual summary of most significant information. If document includes a significant bibliography or literature survey, mention it here.) A failed piston rod and rod end from a DC-8 aircraft main landing gear retract cylinder assembly was submitted to the NBS Mechanical Properties Section for examination. The threads of both of the mating parts were severely corroded and had suffered rather severe mechanical damage. The mechanical damage of the threads appeared to be the result of the failure rather than the cause of the failure. A large portion of the fracture surface had been damaged by an apparent rubbing action. Dimpled rupture was the primary feature exhibited by the undamaged portion of the fracture surface. An anti-seize compound with a molybdenum disulfide base was reportedly used on the threads when the components were in service, but no molybdenum was detected in a chemical analysis of the corrosion product. Of those thread dimensions checked, the root radius of the rod end did not appear to meet specifications.			
17. KEY WORDS (six to twelve entries; alphabetical order; capitalize only the first letter of the first key word unless a proper name; separated by semicolons) Aircraft landing gear; corrosion; dimpled rupture; ductile fracture.			
18. AVAILABILITY <input type="checkbox"/> Unlimited <input checked="" type="checkbox"/> For Official Distribution. Do Not Release to NTIS <input type="checkbox"/> Order From Sup. of Doc., U.S. Government Printing Office Washington, D.C. 20402, SD Cat. No. C13 <input type="checkbox"/> Order From National Technical Information Service (NTIS) Springfield, Virginia 22151	19. SECURITY CLASS (THIS REPORT) UNCLASSIFIED	21. NO. OF PAGES 29	
20. SECURITY CLASS (THIS PAGE) UNCLASSIFIED		22. Price	





